PLASMA
DIAGNOSTICS

Measurements of the Electron Distribution Function in the AMBAL-M Startup Plasma by an Electrostatic Analyzer

T. D. Akhmetov, V. I. Davydenko, and S. Yu. Taskaev

Budker Institute of Nuclear Physics, Siberian Division, Russian Academy of Sciences,
pr. akademika Lavrent'eva 11, Novosibirsk, 630090 Russia

Abstract—The electron distribution function over longitudinal energies in the startup plasma of the end cell of the AMBAL-M device is measured with a small-size movable electrostatic analyzer. It is found that, in the region where a substantial longitudinal current flows, the electron distribution function over longitudinal energies has a plateau in the 150–350-eV energy range. © *2000 MAIK "Nauka/Interperiodica"*.

1. INTRODUCTION

A hot startup plasma with a diameter of 20 cm, a density of $\sim10^{13}$ cm^{-3}, an electron temperature of 50 eV, and an ion temperature of 200 eV is obtained in the end cell of the AMBAL-M device [1]. The plasma is produced by a gas-discharge plasma source located beyond the magnetic mirror. The specific feature of the obtained plasma is a ~1-kA longitudinal electric current flowing in the axial region [2]. To determine the heating and current-drive mechanisms, it is necessary to carry out direct measurements of the electron distribution function in the mirror system. The results of reconstructing the electron distribution function from the current–voltage characteristics of a Langmuir probe [3] located in a hot plasma lead to ambiguous interpretation.

The goal of this work is to measure the electron distribution function in the end cell of the AMBAL-M device by a small-size electrostatic energy analyzer specially designed for this purpose.

Similar energy analyzers have already been used for local measurements of the longitudinal electron current in reversed-field pinches [4–6]. These measurements demonstrated the possibility of using such energy analyzers to determine the electron distribution function over longitudinal energies.

2. DESCRIPTION OF THE ANALYZER

The schematic of the end cell of the AMBAL-M device and the position of the analyzer in the mirror system are presented in Fig. 1. The analyzer is attached to a ceramic tube and is inserted into the plasma with the use of a positioner. The analyzer (Fig. 2) consists of two symmetric sections placed inside an insulating case made of boron nitride. Each of the analyzer sections consists of an input diaphragm with a small aperture, an

analyzing diaphragm, and a collector. The thickness of the input diaphragm made of niobium is 1 mm, and the diameter of the input aperture is 0.3 mm. The analyzing diaphragm has a thickness of 2 mm and an aperture diameter of 1 mm. The centers of the apertures of both diaphragms lie on the axis directed along the magnetic field. The diameters of the electrode apertures were chosen taking into account the energy of ions and electrons in the measurement region.

The measurement method is based on the violation of quasineutrality in the small input aperture, whose diameter is comparable with the Debye length. The ion flux into the analyzer is attenuated due to the relatively
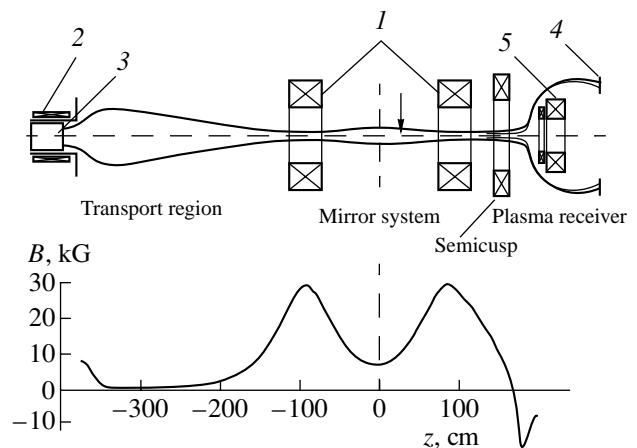

Fig. 1. Schematic of the end cell of the AMBAL-M device: (*1*) coils of the mirror system, (*2*) plasma-source solenoid, (*3*) plasma source, (*4*) plasma receiver, and (*5*) semicusp coils. The position of the analyzer is marked with an arrow. At the bottom, the profile of the magnetic field on the axis is shown.

large thickness of the input diaphragm. Since the ion Larmor radius ($\rho_i \approx 2.5$ mm) in the region where the analyzer is located is substantially larger than the diameter of the input aperture, for the chosen diaphragm thickness, most of the ions fall on the wall of the aperture and do not enter the analyzer. On the other hand, the characteristic electron Larmor radius ($\rho_e \approx 0.025$ mm) is less than the aperture size, so that the electrons pass freely into the analyzer along the magnetic field lines. When the analyzer is inserted into the plasma, the insulated input diaphragm acquires a ~2.5–$3T_e/e$ negative charge with respect to the space potential, so that the current to the input diaphragm is equal to zero. This potential substantially reduces the plasma electron flux through the input aperture. Therefore, the analyzer in fact measures the distribution function of superthermal electrons with energies exceeding 2.5–$3T_e$. The energy analysis of the electrons entering the analyzer is carried out by applying a negative potential to the analyzing diaphragm with respect to the input diaphragm. In order to suppress secondary electron emission from the collector and reject a small portion of ions entering the analyzer because of their small transverse energy, a positive (with respect to the input diaphragm) potential is applied to the collector. The numerical solution of the Laplace equation shows that, for the –100-V potential of the analyzing diaphragm and +90-V potential of the collector, the retarding potential on the axis is –99.6 V. Therefore, in the absence of the electron space charge in the aperture, the retarding potential is approximately equal to the potential of the analyzing diaphragm. The current to the collector is measured with the use of a resistor placed between the input diaphragm and the collector. The electron distribution function $f(U) \propto -\partial j(U)/\partial U$ over longitudinal energies can be obtained by differentiating the measured dependence $j(U)$ of the collector current on the retarding voltage.

3. RESULTS OF MEASUREMENTS

The measurements were carried out in the axial plasma region in the single- shot regime. The shot-to-shot reproducibility of the plasma parameters was 5–10%. In Fig. 3, the oscillograms of the collector current of the analyzer section that faces the plasma source are shown at different values of the retarding potential. It is seen that an increase in the retarding potential results in a monotonic decrease in the collector current. To find the current as a function of the retarding potential, we averaged the current over three 160-μs time intervals, which are marked by the Roman numerals in Fig. 3. In the dependences obtained (see Figs. 4a–4c), most of the parts of the curves are well approximated by straight lines; this is evidence that there is a plateau in the electron distribution function up to energies of 180, 160, and 60 eV, respectively, with a further drop as the energy increases by 50 eV.
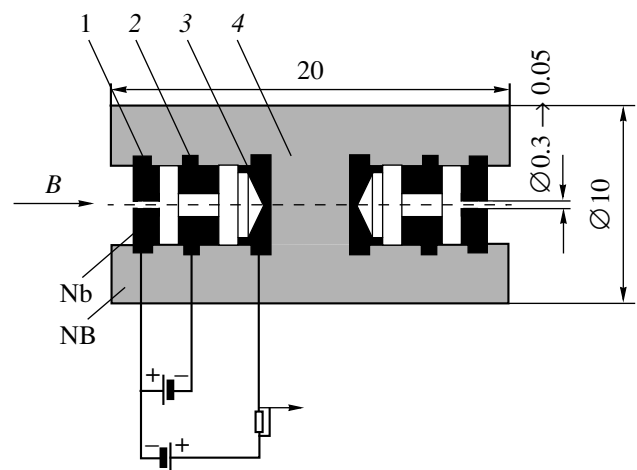
Fig. 2. Schematic of the energy analyzer: (*1*) input diaphragm, (*2*) analyzing diaphragm, (*3*) collector, and (*4*) insulating case.
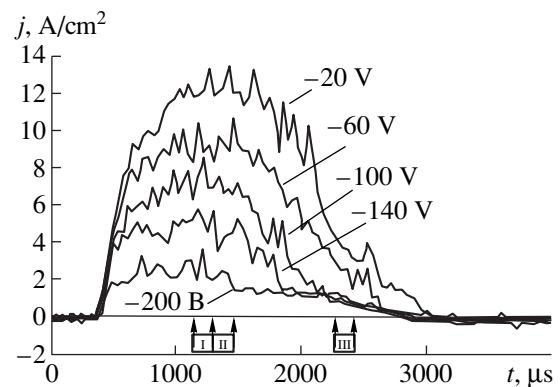

Fig. 3. Oscillograms of the collector current at different retarding potentials. The analyzer is located on the axis and faces the plasma source.

As was noted above, the distribution function can be found by differentiating the experimental dependence $j_{exp}(U)$. However, in this case, the measurement errors lead to undesirable distortion of the sought-for functions. In order to eliminate these errors, the experimental curves should be carefully smoothed beforehand. Therefore, we chose another procedure that also allows evaluation of the distribution function by the measured current provided that the distribution function permits an analytical approximation with several free parameters. For simplicity, we assume that the measured current can be represented as a sum of contributions from the electrons with the Maxwellian distribution over longitudinal energies and an electron beam with a finite temperature. The thermal electrons in the mirror system are described by the Maxwellian distribution function $j_{maxw} = c_m\exp(-\varepsilon/T_m)$, and the beam is given by the Maxwellian distribution shifted by the longitudinal velocity,

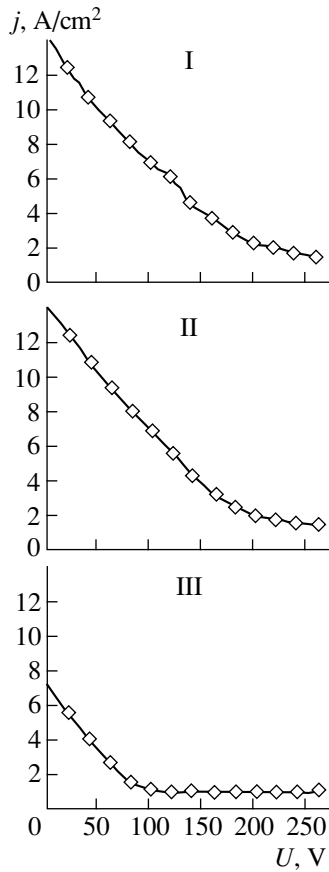**Fig. 4.** The current as a function of the retarding potential for three time intervals (I, II, and III) shown in Fig. 3.
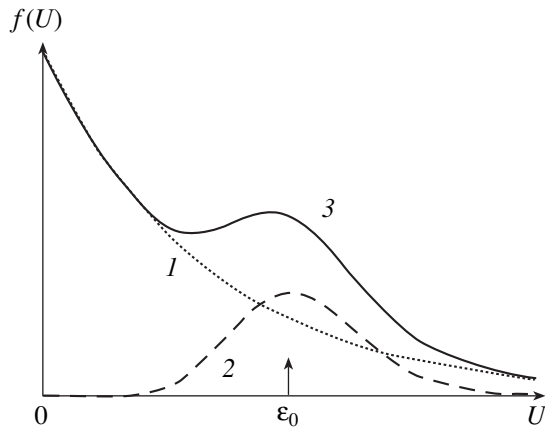

Fig. 5. Model electron distribution function: (*1*) Maxwellian distribution function $f_{\mathrm{max}\,w}(U)$, (*2*) fast-electron distribution function $f_{\mathrm{fast}}(U)$, and (*3*) total distribution function $f(U) = f_{\mathrm{max}\,w}(U) + f_{\mathrm{fast}}(U)$.

$f_{\mathrm{fast}} = c_f \exp(-(\sqrt{\varepsilon} - \sqrt{\varepsilon_0})^2/T_f)$. Here, c_m and c_f are constants determining the densities of Maxwellian and fast electrons; T_m and T_f are the temperatures of these two electron species, respectively; ε is the longitudinal

energy ($\varepsilon = m v_{\parallel}^2/2$); and ε_0 is the average longitudinal energy of the beam electrons. These functions and their sum are presented in Fig. 5. The sought-for parameters c_m, c_f, T_m, T_f, and ε_0 are found by minimizing the sums of squared deviations of the calculated current from the measured current with respect to the free parameters at different voltages. This procedure resulted in the following estimates for the electron energy characteristics: the temperature of the Maxwellian electrons is 100, 80, and 30 eV for the I, II, and III intervals in Fig. 3, respectively; the beam-electron energy is 150, 135, and 60 eV, respectively; the beam electron temperature is ~3 eV in all cases; and the fast-electron density is at least one order lower than the density of the warm Maxwellian plasma. Note that these solutions give somewhat overestimated current values at retarding potentials below 50 eV. Presumably, the low temperature of the beam electrons is explained by the cooling effect (the decrease in the mean-square deviation of the particle velocity from the averaged directional velocity) during the particle acceleration. This effect shows up when the electrons move in the accelerating ambipolar electric field from the input magnetic mirror to the center of the device.

The retarding curve for the analyzer section facing the plasma receiver is shown in Fig. 6. In this case, at the zero retarding potential, the collector current is approximately three-and-a-half times below the current in the case considered above. As before, the electron current flowing into the analyzer is suppressed at retarding potentials up to 200 V. In this case, the electron flux into the analyzer can be related to both the partial reflection of fast electrons by the output magnetic mirror and the superthermal Maxwellian electrons.

Although the measurements show the presence of a plateau in the electron distribution function over longitudinal energies, there are two factors that affect the measurement accuracy. First, the retarding potential applied to the analyzing diaphragm leads to a proportional increase in the potential of the input diaphragm. Thus, when the retarding potential was –200 V, the potential of the input diaphragm increased by 80 V. This effect is similar to the behavior of a double probe in a plasma when the voltage is applied across the interelectrode gap. However, it is difficult to explain the increase in the potential of the input diaphragm quantitatively. Actually, the value of the retarding potential is less than the voltage between the input and analyzing diaphragms. It is found that the dependence of the retarding potential U_{repel} on the potential of the analyzing diaphragm U_d is close to linear: $U_{\mathrm{repel}} \approx 0.6 U_d$. Therefore, the retarding curve can be corrected so that its shape remains almost unchanged.

Another factor affecting the accuracy is the electron space charge. The decrease in the potential on the axis in the input aperture is associated with this space charge and is estimated as $\delta\varphi \approx \pi r^2 ne$. Assuming the
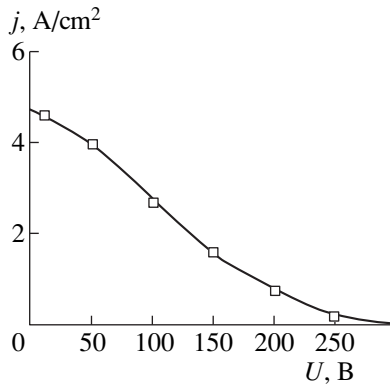
Fig. 6. Retarding curve for the analyzer section facing the plasma receiver.

average electron energy to be 60 eV, we obtain that, for the current density $j \approx 15$ A/cm^2, the density of the electron flow is $n \approx 2 \times 10^{11}$ cm^{-3} and the decrease in the potential on the axis is $\delta\varphi \approx 20$ V. A certain measurement error can also be introduced by the radial nonuniformity of the potential.

In order to carry out more accurate measurements, the aperture diameter of the input diaphragm was reduced to 0.05 mm. In this case, a –200-V retarding potential leads to only a 10-V increase in the potential of the input diaphragm. Hence, we can say that the potential of the analyzing diaphragm has no effect on the potential of the input diaphragm and that it is actually the retarding potential. At the zero potential of the analyzing diaphragm, a decrease in the input aperture area by a factor of 36 resulted in a decrease in the collector current by a factor of 100. This extra decrease in the current is associated with the fact that the radius of the input aperture in this case is equal to the Larmor

radius of electrons with a 50-eV transverse energy, so that not all of the electrons enter the analyzer. Such a small input aperture of the analyzer cuts off not only the ions, but also the electrons with high transverse velocities. This selection emphasizes the contribution from beam electrons with a small transverse temperature. Since the recorded current decreases 100-fold, the space-charge potential also decreases 100-fold and its influence on the measurement accuracy becomes negligible.

Figure 7a shows the dependence of the collector current on the retarding potential, which was measured by the analyzer with the reduced input aperture. Although the dispersion of the experimental points increased because of the decrease in the collector current, it is seen that the electron distribution function is fairly broad and non- Maxwellian. The dispersion of the experimental points introduces some uncertainty in drawing the smooth curve through these points (this curve should be differentiated with respect to the retarding potential in order to obtain the distribution function). As an example, we drew two curves through the experimental points. Figure 7b shows two electron distribution functions over longitudinal energies for two curves drawn through the experimental points. It is seen that, in both cases, the electron distribution function has a plateau in the energy range from $e\varphi_{fl}$ to $e\varphi_{fl} + 200$ eV. Assuming that $e\varphi_{fl} \approx 3T_e \approx 150$ eV, we can state that the plateau is located in the 150–350-eV range of the electron longitudinal energy.

To understand the influence of superthermal plasma electrons, we carried out measurements at a radius of 6 cm (outside the region ~4 cm, where the longitudinal current flows) using the analyzer with the reduced aperture. The results are presented in Fig. 8. At this radius, the bulk-plasma parameters are almost the same as on the axis, but the longitudinal current is absent. The data
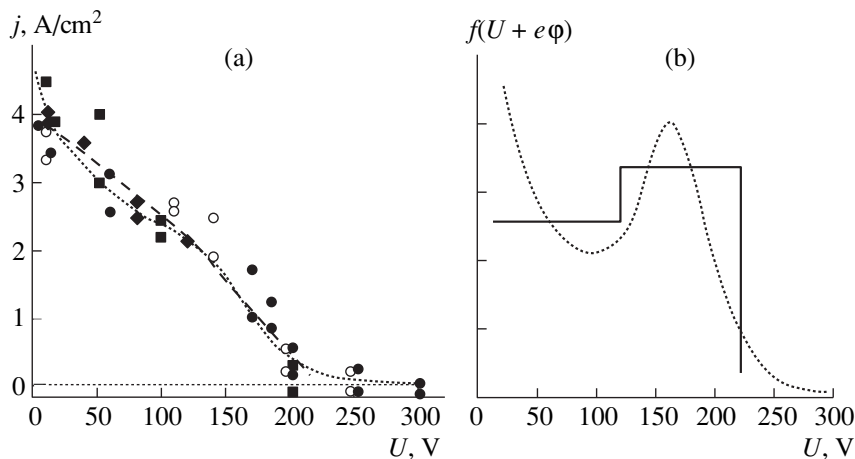

Fig. 7. (a) The retarding curve for the analyzer with a reduced input aperture and (b) the electron distribution functions over longitudinal energies obtained from dashed and dotted curves in Fig. 7a. Averaging is performed over the 1–1.5-ms time interval. The results of different series of measurements are shown by different symbols.
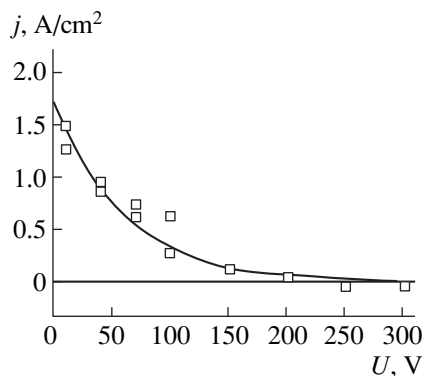
Fig. 8. The retarding curve for the analyzer positioned at a 6-cm radius. The solid line shows the retarding curve for the Maxwellian electron distribution with a 60-eV temperature.
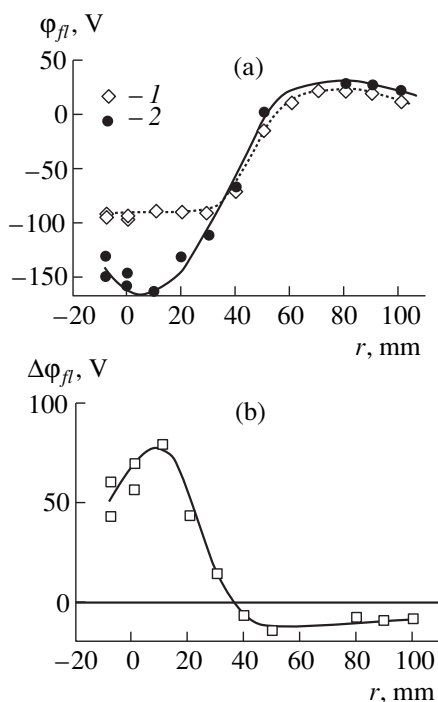

Fig. 9. (a) Radial profiles of the floating potential of the analyzer input diaphragms facing (*1*) the plasma source and (*2*) plasma receiver and (b) their difference.

approximately the same contribution to the current from the Maxwellian and beam electrons.

In addition, we measured the radial profiles of the floating potentials of both input diaphragms, one of which faced the plasma source and the other one faced the plasma receiver. The results are presented in Fig. 9. The profile of the potential difference between the diaphragms shows that the electron distribution function in the axial region is anisotropic. As would be expected, this region coincides with the region where the current flows that was previously detected by a magnetic probe [2].

4. CONCLUSION

A small-size electrostatic electron-energy analyzer is designed and used to measure the electron distribution function over longitudinal energies in the end cell of the AMBAL-M device. It is found that the distribution function has a plateau in the 150–350- eV range in the current-carrying channel of the mirror system and is Maxwellian (with a temperature of 60 eV) outside this channel. The data obtained can be used to carry out numerical simulations of the generation of electrons carrying the current in the transport region between the plasma source and the mirror system.

REFERENCES

1. T. D. Akhmetov, V. S. Belkin, E. D. Bender, *et al.*, Fiz. Plazmy **23**, 988 (1997) [Plasma Phys. Rep. **23**, 911 (1997)].
2. T. D. Akhmetov, V. I. Davydenko, A. A. Kabantsev, *et al.*, Fiz. Plazmy **24**, 1065 (1998) [Plasma Phys. Rep. **24**, 995 (1998)].
3. S. Yu. Taskaev, Preprint no. 95-92, IYaF SO RAN (Institute of Nuclear Physics, Siberian Division, Russian Academy of Sciences, Novosibirsk, 1995).
4. J. C. Ingraham, R. F. Ellis, J. N. Downing, *et al.*, Phys. Fluids B **2**, 143 (1990).
5. M. R. Stoneking, S. A. Hokin, S. C. Prager, *et al.*, Phys. Rev. Lett. **73**, 549 (1994).
6. Y. Yagi, V. Antoni, M. Bagatin, *et al.*, Plasma Phys. Controlled Fusion **39**, 1915 (1997).

Translated by A. D. Smirnova

presented in Fig. 8 are well approximated by the Maxwellian distribution with a 60-eV temperature. For the zero retarding potential, the collector current dropped 2.5 times compared to that measured on the axis, which is explained by the absence of fast electrons. Thus, we can conclude that the previous measurements showed